ROBOTIC PLATFORMS FOR QUALITATIVE AND QUANTITATIVE REAL-TIME ANALYSIS

BY

FAN (LUKE) YANG

A THESIS SUBMITTED IN PARTIAL FULFILLMENT OF THE

REQUIREMNETS FOR THE DEGREE OF

BACHELOR OF SCIENCE

IN

THE FACULTY OF SCIENCE

(COMBINED HONOURS CHEMISTRY AND MATHEMATICS)

THE UNIVERSITY OF BRITISH COLUMBIA

(VANCOUVER)

APRIL 2021

©FAN (LUKE) YANG 2021

ABSTRACT

Research chemistry experiments include a variety of repetitive and laborious tasks that can be accomplished using automated laboratory instruments. One of the limitations of current workflows involving these automated instruments is that instrumental commands are usually needed to be pre-planned and executed in a fixed order. Human intervention remains crucial to driving workflows that require decision-making regarding current experimental states. The ability to extract, analyze, and respond to the current experimental states are paramount to build a self-driven workflow with the automated instruments. We developed two automated robotic platforms respectively featured with a qualitative and a quantitative method of real-time feedback analysis. For the qualitative analysis, we developed an automated solubility screening system by implementing the recognition of chemical dissolution. The recognition of chemical dissolution is achieved by turbidity measurement using computer vision. For the quantitative analysis, we automated a two-step, carbonyldiimidazole-activated, amide bond formation using arbitrary carboxylic-acid-amine pair. The transition between the two steps is perceived by auto-HPLC sampling sequences, where the disappearance of the carboxylic acid reagent peak reflects the endpoint of the first step. To promote the remote accessibility and flexibility of the platforms, we integrated Slack as a laboratory assistant to notify the experimenter of the workflow progress and to control the platforms using keyword commands.

TABLE OF CONTENTS

LIST OF FIGURES

LIST OF TABLES

ACKNOWLEDGEMENTS

I want to offer my most genuine gratitude to Dr Jason Hein for giving me this incredible opportunity to be involved in these amazing projects. Great thanks to Parisa Shiri for being a wonderful mentor. I also appreciate the supports from all members in the Hein Lab, especially Sean Clark for the programming support, Yusuke Sato and Junliang Liu for experimental support.

1. INTRODUCTION

In research laboratories, many experimental techniques involve repetitive and time-consuming procedures. Each procedure may only consist of low complexity but often requires significant attention from the experimenter[1]. The inevitability of performing these procedures results in inefficient uses of the research time thus decreases the researcher's productivity[2]. To solve this situation, automated laboratory instruments can be deployed to perform unsupervised experimental procedures, allowing the experimenter to utilize their research time more productively. During the last century, advancement in laboratory instruments has brought multiple benefits towards research, teaching, and industry[1-3]. Efforts of building the bridge between laboratory instruments and computer programs have been made to reach control integration[3-6]. Beyond simply controlling instruments using pre-programmed software, workflows have been designed combining one or more programmable instruments with capabilities to accomplish elementary experimental tasks. Due to the modular characteristic of these programmable instruments, a robotic arm is generally deployed as the core of experimental workflows for inter-module communication and transportation[7-9]. The actions of the robotic arm simulate the actual operations performed by the experimenter[7,9]. By appropriate instrumental command arrangement, an integrated platform involving the robotic arm and the programmable instruments enables scientists to reduce hands-on experimental time on repetitive procedures and modify the experiment conditions without physically being near the setup[10].

While robotic platforms can carry out experimental procedures in a fixed sequence, handling conditional cases requires the computer algorithm's capability to extract, analyze, and respond to the information of the current experimental state. During an experiment, it is commonly required from the experimenter to observe the noticeable physical changes, such as the transformation of appearance or emission of heat or light[11]. These qualitative descriptions of an experiment can be sufficient in many

circumstances; in particular, the turbidity of a liquid-solid mixture is a key factor that determines the dissolution of a chemical substance. Being able to process the visual feedback on turbidity is essential in driving an automated workflow for solubility testing[10].

Although qualitative feedback can be valuable for analysis when obvious physical effects exist, most organic experiments consist of few or no observable indication of the state of the experiment. In particular, if an experiment involves multiple steps, the transition time point of the preceding and the succeeding step is unknown without quantification. To determine the progress of these experiments, quantitative analysis, such as nuclear magnetic resonance (NMR), ultraviolet-visible spectroscopy (UV-Vis), or high-performance liquid chromatography (HPLC), is often needed. Among these quantitative methods, HPLC stands out to provide a distinctive determination of individual substances regarding their entire structures, and it is applicable to the majority of the organic substances. Being able to automate the HPLC injection sequence and interpret the chromatographic data is essential in driving a multi-step experiment workflow.

In this report, we present two robotic reaction stations that automate titration-like solubility testing and carboxylic-acid-amine coupling reaction. The two reaction stations are designed to be self-driven based on the qualitative and quantitative feedback, obtained using the computer vision module and HPLC direct-inject module. The computer vision module is designed to support turbidity measurement used for solubility testing, and the HPLC direct-inject module functions to recognize, label, and identify appearing and disappearing chemical substances detected as chromatogram peaks. The modules and instrumental control libraries are developed using Python programming language. In addition, the real-time monitored data is visualized and reported to the experimenter via Slack, in which the experimenter can also directly control individual modules using keyword commands. This provides enhanced remote accessibility, as well as simplified yet integrated instrumental control.

2. QUALITATIVE FEEDBACK ANALYSIS – SOLUBILITY SCREENING

2.1 Introduction

Solubility is defined as the maximum amount of a chemical substance that can dissolve in a certain amount of solvent under a known temperature when the system approaches its equilibrium. The ability to reliably determine solubility is essential to many research and industry sectors, such as material chemistry and pharmaceutical processing[12,13], where solvent selection is crucial for product formulation and process development[12-15]. One of the most common solubility determination methods is mixing an excess amount of solute with the initial solvent and dosing solvent increments until the mixture reaches a homogenous phase. Though using analytical techniques, such as UV-Vis or HPLC, is useful to determine the concentration of a saturated solution[16], monitoring the turbidity of the solution mixture is a significantly more efficient and convenient method that reflects the dissolution of chemical substances. While it is trivial for the experimenter to distinguish the turbid or non-turbid state, the time interval allowing the system to equilibrate after each solvent addition is can be lengthy. Thus, continuously monitoring the turbidity of a solute-solvent mixture requires a significant amount of attention from the experimenter, and stepwise solvent addition also consumes hands-on research time. The question was raised: "How can we automate this time-consuming endeavour using laboratory automation?". We integrated the liquid handling module, the solid handling module, and computer vision module to construct an automated self-driven solubility screening platform (see Appendix for individual instrumental modules).

2.2 Method

2.2.1 Computer Vision

We developed the HeinSight turbidity module to analyze the graphical feedback obtained from the webcam. The HeinSight is a Python package previously developed by the Hein Lab for automation of general laboratory tasks, which involves visual feedback interpretation[10,25]. The turbidity module of HeinSight is designed to analyze the turbidity of a solution mixture in a given region of interest (ROI). The computer vision algorithm measures the average brightness of the pixels in the ROI and compares them with the result of a known non-turbid solution. In modern research, most turbidity measurements using computer vision are based on constructing comparison libraries[25]; however, the construction of this library requires a complicated instrumental setup and is subjective to the lighting effect. Changes in the ambient brightness may result in measurement errors, thus influence the decision-making of the workflow. In this solubility test setup, we used a dissolved reference adjacent to the measurement vial. Both ROIs from the measurement vial and the reference vial are monitored by a webcam. The monitored results are based on the comparison of the two ROIs to account for the ambient lighting condition.

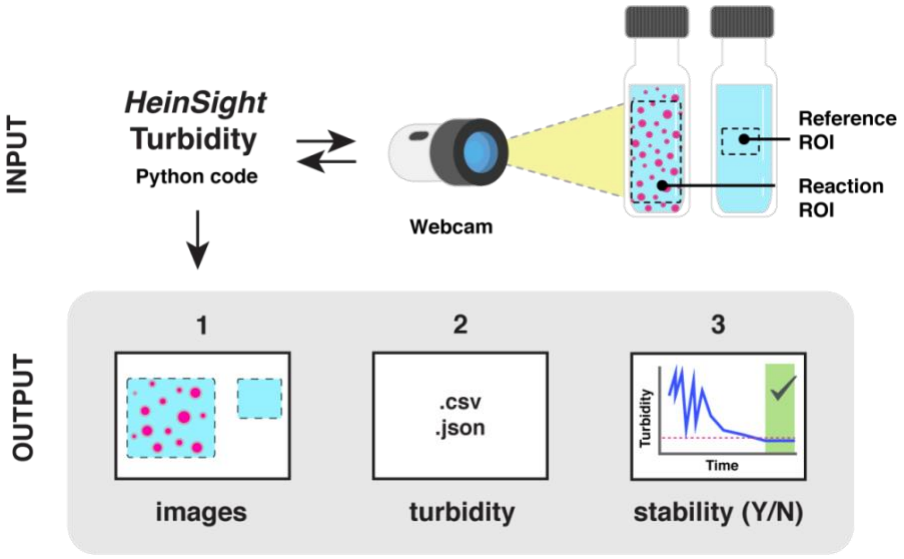

Figure 4: HeinSight turbidity module algorithm

The HeinSight turbidity Python package quantifies the turbidity based on the brightness of the captured images. The turbidity data as time progresses is stored locally, and the trend of turbidity change is analyzed. The data is visualized using a turbidity versus time plot (*Figure 1.3*). In the workflow, an excess amount of the solid analyte is first mixed with the solvent to form a heterogeneous mixture. Small aliquots of solvent are then added attempting to dissolve the heterogenous mixture, which is reflected in the decreasing trend of the turbidity versus time plot. If the analyte turbidity quantity is constant below the measure reference turbidity quantity, the computer decides that the state has changed to dissolved.

2.2.2 Workflow for Qualitative Monitoring

The workflow uses the Quantos automated balance for solid dosing, the VICI selection value for connection, the Tecan Cavro syringe pump for liquid dosing, the IKA stir plate for mixing, and the Kinova robotic arm for vial transfer. See Appendix for detailed instrument descriptions.

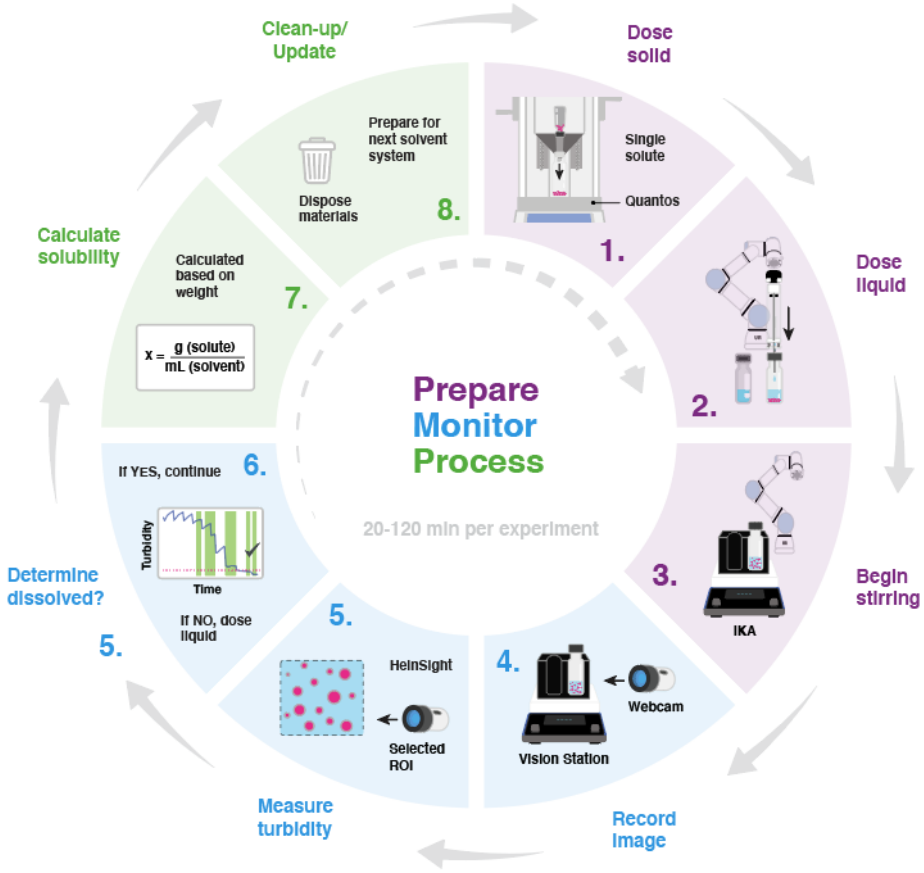

Figure 5: Diagram of the solubility workflow

Preparation

We assembled and arranged them into an automated workflow *(Figure 2)*. After inputting a collection of the desired testing solvents and solids, the robotic arm brings the corresponding dosing head into the Quantos automatic balance. The VICI valve switches to the desired solvent selection port, and Tecan Cavro syringe pump begins initial line priming. With the line filled and needle washed with

the solvent, the robotic arm transfers an empty vial from the vial deck into the gripper station and uncaps the vial. The uncapped vial is then transferred into the Quantos to initialize the dosing sequence for a guessed mass of the solid. The arm then brings the Sampleomatic to fill the vial half-full (0.5 mL) of the solvent. When the liquid and solid dosing are complete, the arm transfers the vial to the gripper station to cap. Afterward, the capped vial and a clear dissolved reference are transferred to the vision station. Contemporarily, IKA stir plate is initiated at a stir rate of 250 revolutions per minute (RPM), and the webcam begins to monitor the turbidity of the measurement vial using the computer vision module.

Monitoring and Processing

Based on the graphical feedback of the vision station, the computer decides whether the solid has dissolved by comparison between the measurement vial and the reference vial. The workflow has different methods of handling depending on the observed dissolution condition (*Figure 3*).

If the reaction mixture appears clear after 5 minutes without any subsequential liquid additions, the substance is likely to have a greater solubility than the current solid-solvent ratio. In this case, the turbidity monitoring terminates, and the arm brings the measurement vial back to the vial deck. In the next run, the Quantos will dose solid mass twice as much as the current run.

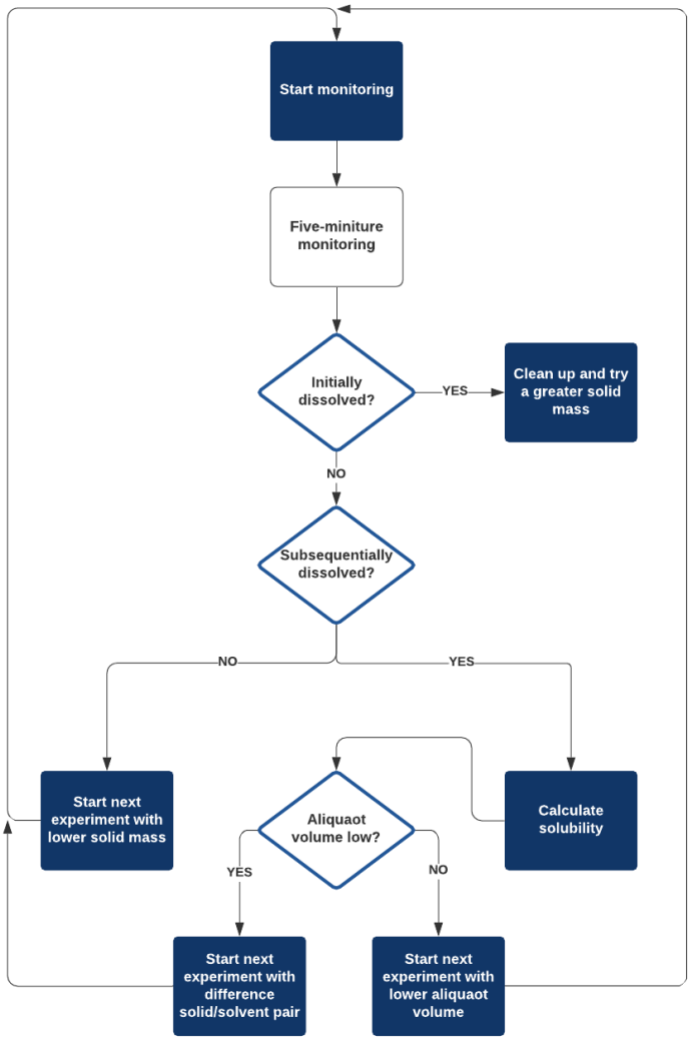

Figure 6: Decision-making flowchart for solubility sequence

If the reaction mixture appears turbid, the substance is likely to have lower solubility than the current solid-solvent ratio. After 5 minutes of stirring and monitoring, if the mixture stays turbid, the robotic arm grabs the Sampleomatic and dose a 0.04 millilitres aliquot of solvent. This procedure is repeated until the maximum capacity of the vial (1.2 millilitres) is exceeded, or the mixture no longer appears turbid. If the maximum capacity of the vial is exceeded and the mixture appears turbid, it is likely that the solubility of the solid is too low to dissolve the input mass within the volume of 1.2 millilitres. In the next run, the Quantos will dose solid mass half as the current run. If the mixture becomes clear as more solvent gets added, the vial is brought back to the vial deck, and a calculation is run to compute the solubility result of the current run. In the next run, aliquots of 0.01 millilitres will be applied to obtain a more precise solubility result.

Once three runs of the solubility tests with 0.01-millilitre step addition are complete, the computer records the solubility of this solvent-solid pair as the average of the three results. If there are more than one input solids or solvents, the workflow repeats the procedure with an untested solid-solvent pair until all are tested.

2.3 Results and Discussion

2.3.1 Data Plots

Caffeine and tetrabenazine (TBZ) were selected as the analyte for the solubility testing using the automated robotic platform. *Figure 4* illustrate the ideal examples of solubility tests while dissolving the excess caffeine and TBZ. The blue curved indicate the quantified turbidity data of the solid-liquid mixture produced by the computer vision algorithm. The orange dashed lined indicate the turbidity level of the dissolved reference solution, which is used for the assessment of the reaction vial's dissolution

condition. The green shaded regions indicate the turbidity data is relatively constant, implying that the system has reached equilibrium.

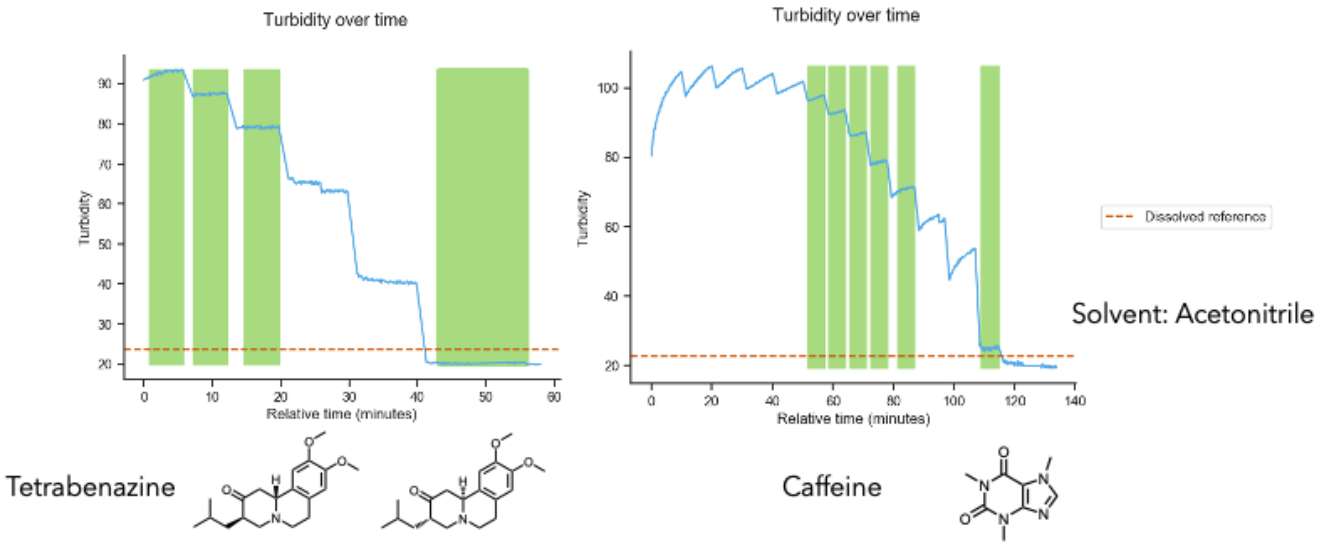

Figure 7: An example of the ideal turbidity plot using TBZ and Caffeine

Since the workflow is designed to have an excess of the solute added at the initial stage, a general decreasing stair-like tendency is expected. The turbidity of the reaction vial consists of a high value when the monitoring starts. The additions of small aliquots of solvent are shown as the steep drops in the plot. After a sufficient amount of solvent is added, the solute dissolves, indicated as the turbidity value of the reaction vial goes below the reference vial turbidity value. Though a similar decreasing behaviour is observed in the plots of both compounds, it can be noticed that the curve of caffeine turbidity over time exhibits an inclining tendency after each solvent addition.

Unlike the turbidity measurement while dissolving TBZ, where a horizontal data curve is observed after each solvent addition, during the dissolution of caffeine, we notice an inclining tendency instead. To ensure this phenomenon does not occur after the measured turbidity goes below the reference turbidity, which may lead to a recovery of high turbidity value after the algorithm categorizes the state as dissolved, we investigated this inclining behaviour using the video recorded by the webcam. Figure 5 shows the three stages when an aliquot of solvent is dosed into the reaction vial. *Figure 5[a]*

indicates the state before adding the solvent aliquot when the solid-liquid mixture appears more turbid. *Figure 5*[b] shows the image taken just after the addition of the solvent. The addition of the solvent dissolves a portion of the caffeine in solid form, which results in a slightly less turbid appearance. *Figure 5*[c] shows the image of the vial after a few minutes of stirring. We notice the constant stirring grinds the solid caffeine into a finer particle form. This grinding effect increases the total amount of solid fragments, but the existing solvent volume is not sufficient to dissolve the fragmented solid. Thus, the reaction vial appears more turbid while stirring, reflected as the increasing turbidity measurement in *Figure 4*. Given the understanding of that, since the solid is completely dissolved when the turbidity goes below the reference line, we conclude that the turbidity does not increase after the computer confirms the dissolution of the solid.

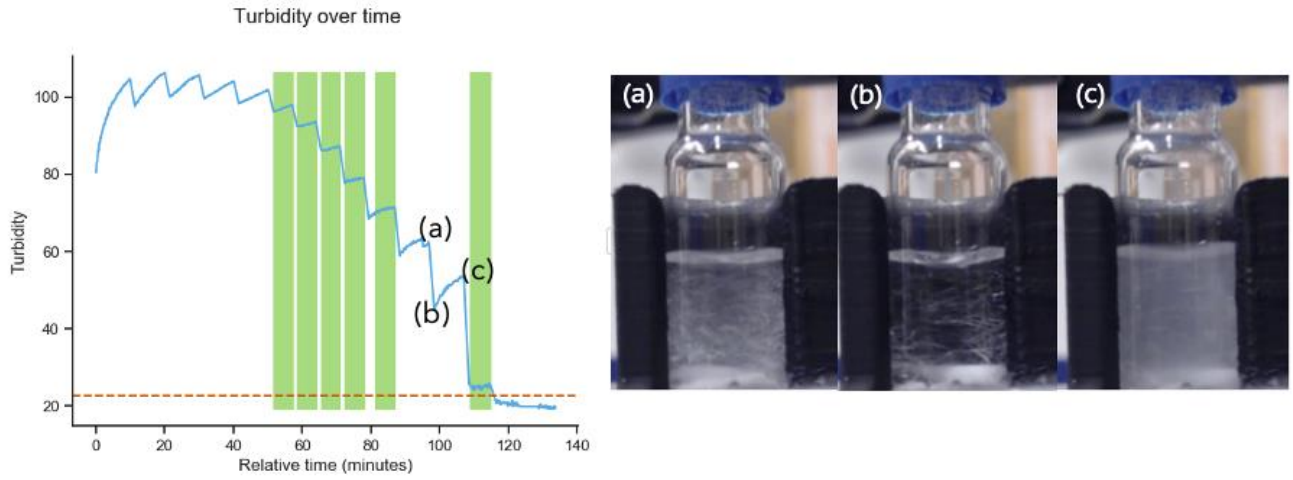

Figure 8: (a) Image of the vial before adding the solvent aliquot. (b) Image of the vial after adding the solvent aliquot. (c) Image of the vial after stirring for awhile

To ensure that the automated platform achieves the same experimental goal as the experimenter, we manually performed solubility tests for TBZ under the same experimental condition. The comparison between data obtained manually and using the automated platform is presented for TBZ (*Table 1*).

Solvent	Ethanol	Isopropanol	Ethyl Acetate	Methanol	Acetonitrile	Acetone
Robotic ± SE (mg/mL)	16.18 ± 0.79	9.72 ± 0.18	64.54 ± 1.75	24.51 ± 0.21	64.54 ± 1.75	87.97 ± 0.88
Manual (mg/mL)	16.82	9.74	65.29	24.63	65.29	88.34

Table 2: Solubility data comparison between the robotic platform and manual procedures for TBZ (SE: Standard Error)

We observe a great consistency between the results produced from the robotic platform and manual solubility results. The manually obtained data fall within the range given by the mean value and standard error (SE) from data obtained using the robotic platform. This consistency indicates that using the robotic platform achieves the experimental goal as hands-on procedures. Noticeably, the manual data appears to be slightly higher than the mean of the robotic data. We hypothesize that using the needle for fixed volume dispense may form an incomplete droplet at the end. The incomplete droplet may not enter the system but stay on the needle tip, so that less solvent is added to the system than expected. Thus, the solubility results appear lower than the manual results. This hypothesis indicates that there exists a systematic error in small solvent addition that may be solved in the future.

2.3.2 Slack Integration

Remote accessibility often appears as a corollary feature of automation[2,25,27]. Since the experiment running on the self-driven robotic platform can take from 20 minutes up to 2 hours, and the researcher is not required to be present in the laboratory, it is advantageous to develop an online update system to

inform the reaction progress. In addition, chemists without a coding background or who are not trained to use the programmable hardware may find it challenging to utilize the automated reaction workflow. The instrumental control needs to be simplified for application towards general chemists. Hence, we integrated Slack as a laboratory assistant to update the real-time monitored data and to deliver the keyword command from the experimenter to the instrumentation.

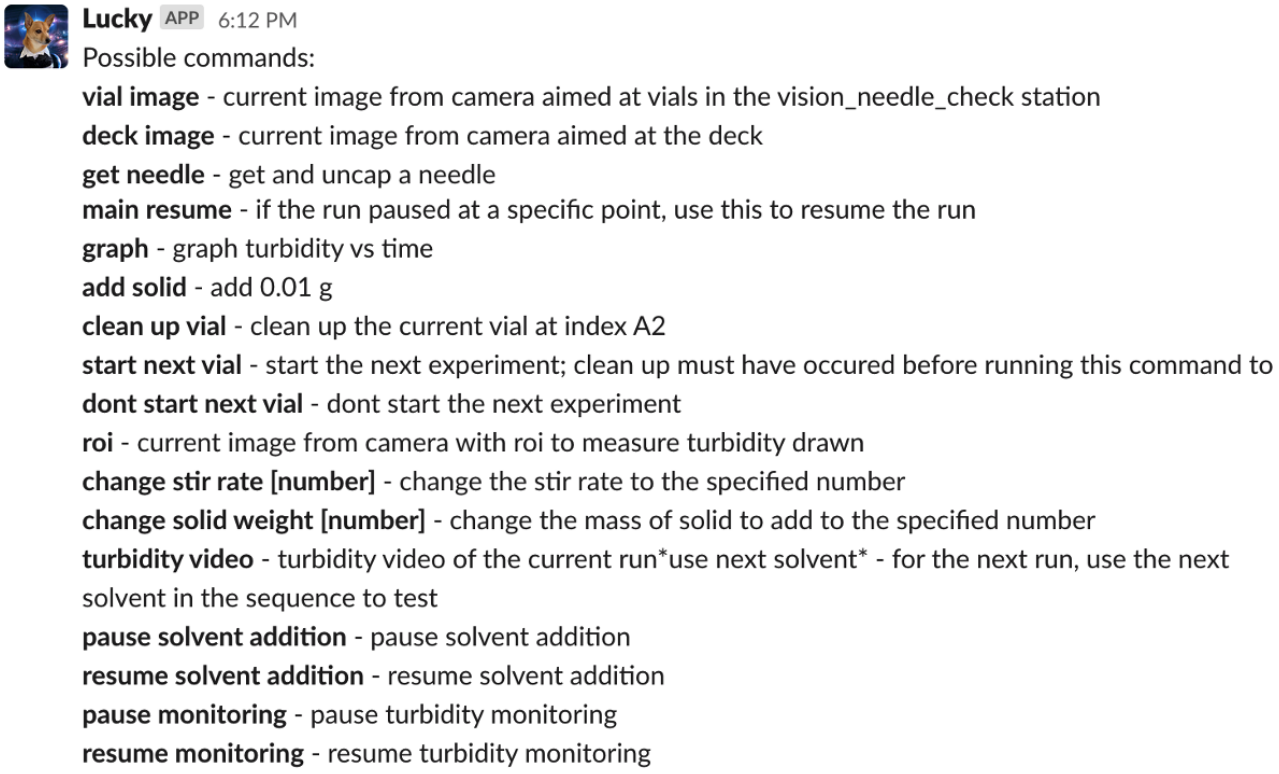

Figure 9: A list of available keyword commands for solubility testing

Figure 6 shows a list of the keywords that are recognized by the Slack laboratory assistant, followed by a short description of each keyword's function. The Slack laboratory assistant allows the experimenter to modify the reaction while the workflow is running. In particular, the experimenter can change the initial solid dosing weight. The ability to change the solid dosing weight becomes practical when the initial guessing of the solute's solubility is significantly different from the true value. Instead of letting the computer algorithm target the appropriate initial dosage by stepwise trials, remote human

intervention can greatly accelerate the convergence to the true value. Furthermore, being able to change the stir rate, pause or resume the workflow is useful in a variety of situations.

The Slack laboratory assistant also provides live reports for the current experimental status. For instance, it automatically notifies the experimenter when the prepare, monitor, and calculate stages initiate and terminate. Using the keyword commands, the experimenter can acquire the images of the deck from different perspectives. The “roi” command proved to be particularly useful combining with the “graph” command. This combination offers a comparison between the real-life image and the computational interpretation. Using these commands, the experimenter can evaluate the accuracy of the turbidity measurement and adjust the configuration of the setup if necessary.

2.3.3 Limitations

The presented solubility testing platform and computer vision module allow the experimenter to perform solubility tests using a titration-like method, and the turbidity of the mixture is measured by quantifying the brightness of pixels in the selected region of interest. While this computer vision method gives a reliable approximation of the turbidity with minimal computational effort, it limits the range of applicable solutes by their physical properties. First, it requires a relatively uniform particle size of the solute, such that under the mixing condition, no clumps of solute are floating above or sinking below the region of interest. Then, a while or while-like appearance is required from the solute, and a colourless dissolved reference is desirable. Using coloured solutes may invert the turbidity comparison, which leads to false decision-making. Though this platform and algorithm are applicable to the majority of organic chemicals, it would be valuable to develop the computer vision algorithm to adapt a larger variety of chemical substances in future modifications.

3. Quantitative Feedback Analysis – Amide Bond Formation

3.1 Introduction

Amide bond formation it is one of the most fundamental organic reactions in synthetic chemistry[17]. The formation of amide bond is critical in pharmaceutical synthesis due to its ability to offer linkages between amino acids, which relevant to around 16% of reactions performed in the pharmaceutical industry[18]. One of the most common amide bond formation strategies is the coupling of a carboxylic acid and an amine via carbonyldiimidazole (CDI) activation[19] (*Figure 7*).

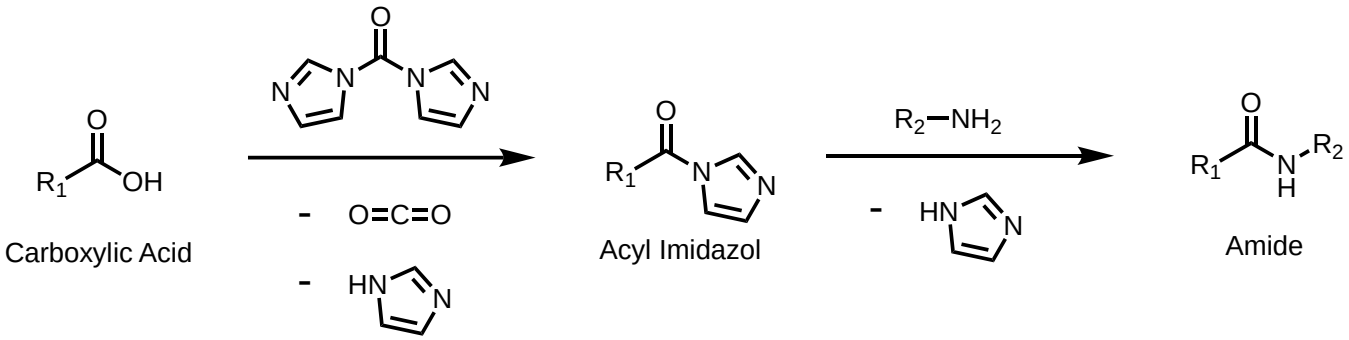

Figure 10: Carboxylic acid and amine coupling via carbonyldiimidazole activation

The CDI activation represents a preferable synthetic route of amide bonds due to the cost-effectiveness of the reagent, mild requirements of reaction condition, and adequate stability of the intermediates[20]. The reaction undergoes two consecutive steps: first, the CDI reacts with the carboxylic acid to form the acyl imidazole intermediate; after the carboxylic acid is completely reacted, the amine is added to react with the intermediate to form the amide product. However, all reagents and the product appear colourless while dissolved, and no noticeable physical change is observed during the reaction. The determination of reaction progress requires validation from analytical techniques.

High-performance liquid chromatography (HPLC) is a powerful analytical technique for substance identification and quantification in analytical chemistry. This technique relies on pumps to

deliver a diluted reaction sample, or the mobile phase through a pressurized column that contains a solid adsorbent packing material, or the stationary phase. Since the interaction between each substance in the mobile and stationary phases is different, substances consist of different flow rates through the column, which are reflected on the chromatogram as separated peaks[21]. Using well-developed HPLC methods, analytes can be differentiated by their characteristic peak retention time under the appropriate chromatographic condition[23]. Also, the quantity of the peak area by integrating the peak intensity over time indicates the proportion concentration of the corresponding substance in the diluted reaction sample. Since the concentration calculated from the chromatogram depends on the dilution factor of the HPLC sample, a known amount of internal standard is usually added to normalize the detected amount of each substance present in the reaction system[22]. By the inert nature of the internal standard, the amount of each substance can be converted from the peak ratios of the analyte peaks to the internal standard peak. While most of the HPLC systems are accompanied by their well-constructed software for peak integration and analysis, the results are subjective to the environmental noises, which may lead to inaccurate integration values or false-positive peak recognition. During the CDI activation, the experimenter is ordinarily required to validate that the carboxylic acid peak disappears, which confirms the completion of the first step. Nevertheless, the manual HPLC sampling and monitoring of every type of carboxylic acid can be laborious and time-consuming[24]. Alternatively, an elongated waiting time for the CDI activation can be set to ensure the completion of the first step, but this method can potentially waste much time on fast-reacting carboxylic acids. With the previously mentioned liquid handling module, we are able to dose reagents without human intervention. However, the transitions from the first step to the second step for new carboxylic acids remain unknown. The question was raised: “How can we determine the completion of the first reaction step and initialize the second reaction sequence?” We

integrated HPLC direct-inject module and HPLC data analysis program to automatically transit between two reaction steps.

3.2 Methods

3.2.1 HPLC Data Processing

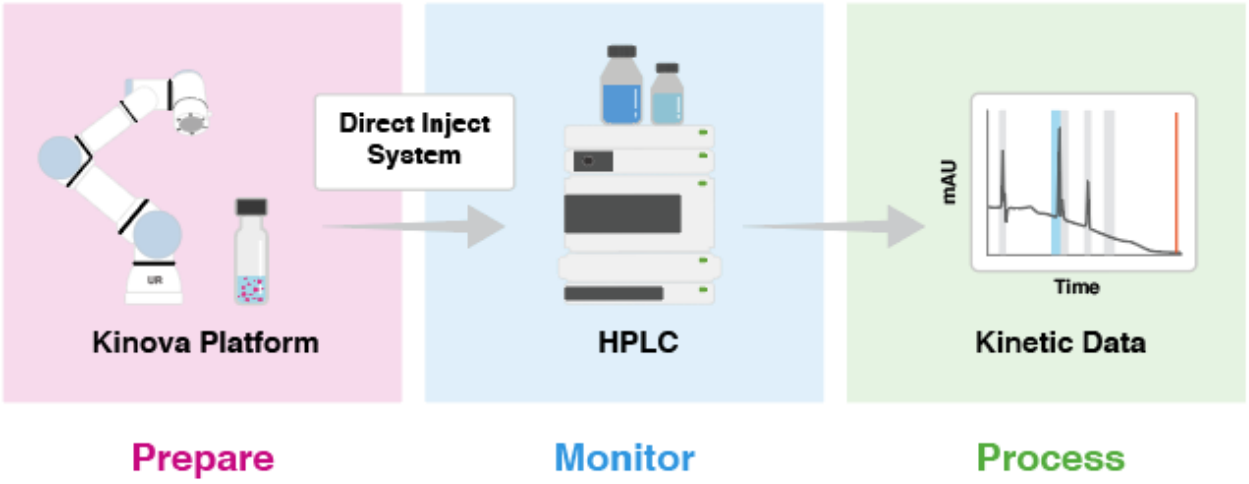

Figure 11: Quantitative analysis diagram

Each time we inject HPLC sample into the Agilent LC system, the LC software processes the detected data and recognizes the appeared peak-like shapes. The characteristic retention times of recognized peaks are recorded, and the areas are computed using the internal integration methods. The data is visualized in the LC software (*Figure 9*) and saved locally in the associated computer. However, the analyzed data includes some unnecessary information. The method of integration is subject to the baseline of the intensity. The error of auto-integration is normally perceived by the experimenter; however, the automated workflow is expected to progress with the least amount of human intervention. We developed an algorithm of HPLC analysis methods to store, calculate, and interpret the raw data.

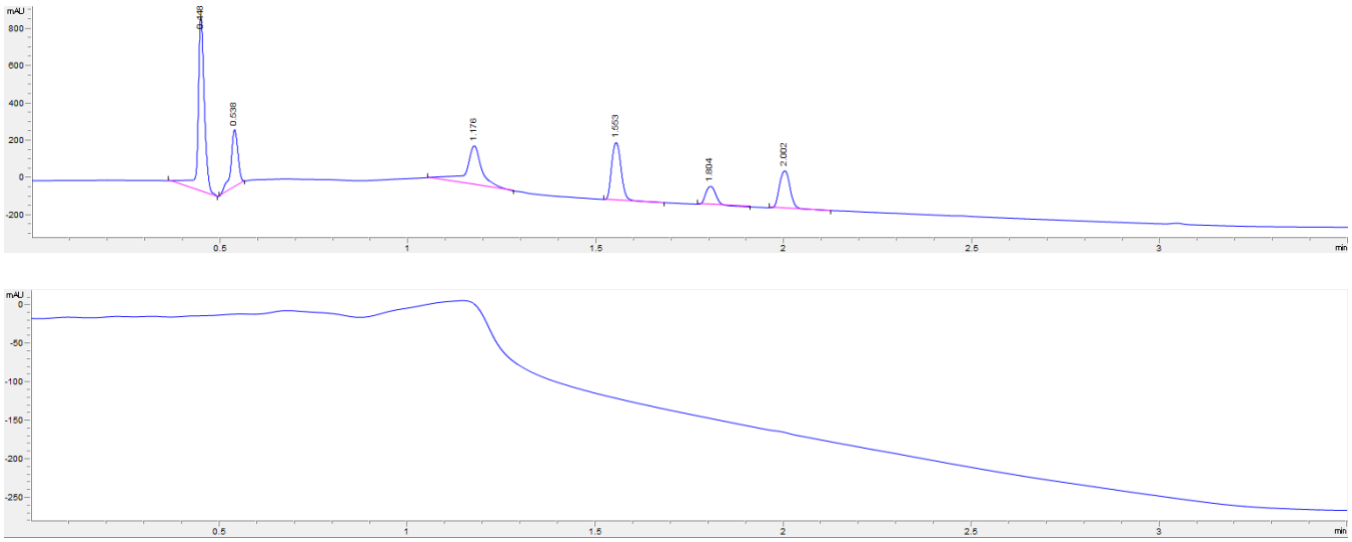

Figure 12: Unprocessed HPLC data from Agilent LC system

In the beginning of each workflow, we run a blank sample to obtain the base time of the HPLC intensity. The result of the blank sample is compared with the subsequential reaction sample to calibrate for the environmental influences. The algorithm uses Python programming language to calculate the difference between the reaction sample signals and the blank sample signals. The difference produces better-behaved data with a flat baseline for the computer to analyze. The algorithm then recognizes data points whose intensities are above a detection limit as a "peak". Because of the flattened behaviour of the baseline, the algorithm chooses the left and right endpoints of the peak to be when the derivative of the peak approaches zero. The peak is then interpolated between the left and right endpoints using the UniversalSpline package from the SciPy library. UniversalSpline is a Python package that performs piecewise interpolations using degree-5 polynomials. It features advanced numerical accuracies while approximating continuous functions. The interpolated function is then integrated to get the numerical result of the peak area.

Since the chromatogram contains signals that indicate the mobile phase travels the length of the column, which is shown in (*Figure 9*) as 0.448 and 0.538, the algorithm discards data before 0.6 mins to avoid recognized noise peaks. Then, a list of detected peak retention times and the corresponding peak

areas are saved in the Python script. During the process of the reaction, each appearing peak is labelled for decision making and data visualization.

3.2.2 Workflow for Quantitative Monitoring

At the start of each workflow, a blank sample is run in the LC system. While the blank sample is being run, the robotic arm moves an empty vial pre-dosed with a stir bar to an available position of the Integrity reaction station (See Appendix for instrumental details). The environment in the Integrity is maintained with a temperature of 25 degrees Celsius and a stir rate of 500 RPM. With the effective mixing condition, the robotic arm uses the Sampleomatic to consecutively dose 5 mL of tetrahydrofuran, 1,3,5-trimethoxybenzene as the internal standard, and one equivalence of the carboxylic acid. In between each reagent addition, the robotic arm takes a sample using the Sampleomatic for HPLC analysis, and the Python script labels the new appearing peak as the name of the previously added reagent. Then, the robotic arm adds two equivalence of the carbonyldiimidazole. Since carbonyldiimidazole cannot be detected by HPLC, and the addition of carbonyldiimidazole initializes the first step of the reaction, a peak of the reaction intermediate, the acyl imidazole is detected. The Python script labels this peak as “intermediate”. The reaction is then monitored in 10-minute intervals. When the acid peak is no longer detected, 50 microlitres of water are dosed to quench the reaction. A 2-hour wait time is set to complete the hydrolysis of carbonyldiimidazole *(Figure 10)*.

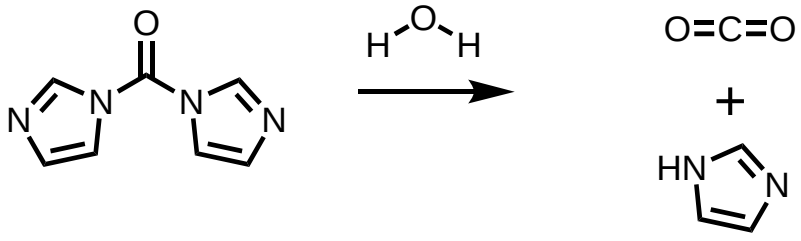

Figure 13: Hydrolysis of carbonyldiimidazole

After the carbonyldiimidazole is hydrolyzed, the robotic arm initiated the second step of the reaction by dosing one equivalence of amine. The second step of the reaction is monitored by HPLC in 10-min intervals, and both amine reagent and amide product peaks are expected in the chromatogram. The algorithm compares the two unlabeled peaks by their increasing or decreasing trend to label them as "product" (amide) and "amine" respectively. The peaks are monitored in 30-minute intervals for next until the concentration of amine and amide approaches constant, which implies the reaction approaches its equilibrium. In that case, the monitoring terminates, and the robotic arm cleans up the deck.

3.3 Results and Discussions

3.3.1 Quantitatively Monitored Data and Comparison

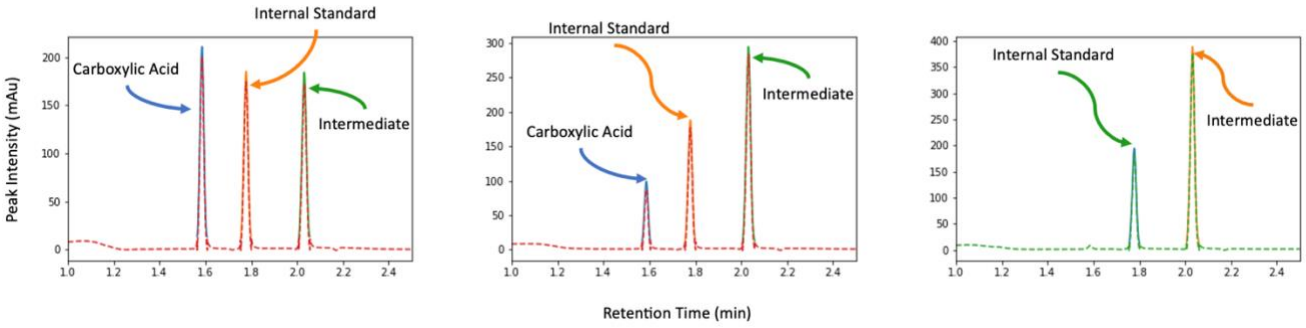

Figure 14: Three chronologically taken samples during the CDI activation

Figure 11 shows an example of the processed HPLC chromatograms of the CDI activation step. Three peaks with their distinct retention time (RT) are monitored, corresponding to the carboxylic acid (RT: 1.59 min), the internal standard (RT: 1.78), and the acyl imidazole intermediate (RT: 2.03). The dashed line indicates the instrumental signals from the HPLC referenced using the blank data. The solid curves indicate the peaks recognized by the algorithm. As the reaction progresses, the intensity and shape of the internal standard peak stay constant due to its inert nature. The size of the acyl imidazole intermediate peak is increasing, suggesting the increase in the concentration of the intermediate. The size of the

carboxylic acid peak is decreasing, and in the third sample (*Figure 11*), the carboxylic acid peak disappears. The decreasing trend of the peak size indicates that the carboxylic acid is being reacted, and the disappearance of the peak implies the completion of the CDI activation.

With different R-group, the carboxylic acid's reaction rate is different for the CDI activation. Traditionally, when the amide bond formation involves a novel carboxylic acid, the CDI activation time length of this carboxylic acid needs to be measured using analytic techniques such as thin-plate chromatography (HPLC) or high-performance liquid chromatography (HPLC). Given that the algorithm can detect and assign each appearing peak to a label, we designed the algorithm to monitor the carboxylic acid peak. During the CDI activation, when the carboxylic acid peak is no longer detected (*Figure 11*^{c}), the 10-minute sampling "loop" stops, and the workflow advances to the next step: CDI hydrolysis. The ability to recognize the endpoint of the CDI activation is important because it greatly reduces the human effort to measure the appropriate reaction wait time, which promotes the applicability of this robotic platform towards arbitrary carboxylic acid type starting materials with maximized reaction efficiency.

3.3.2 Slack Integration

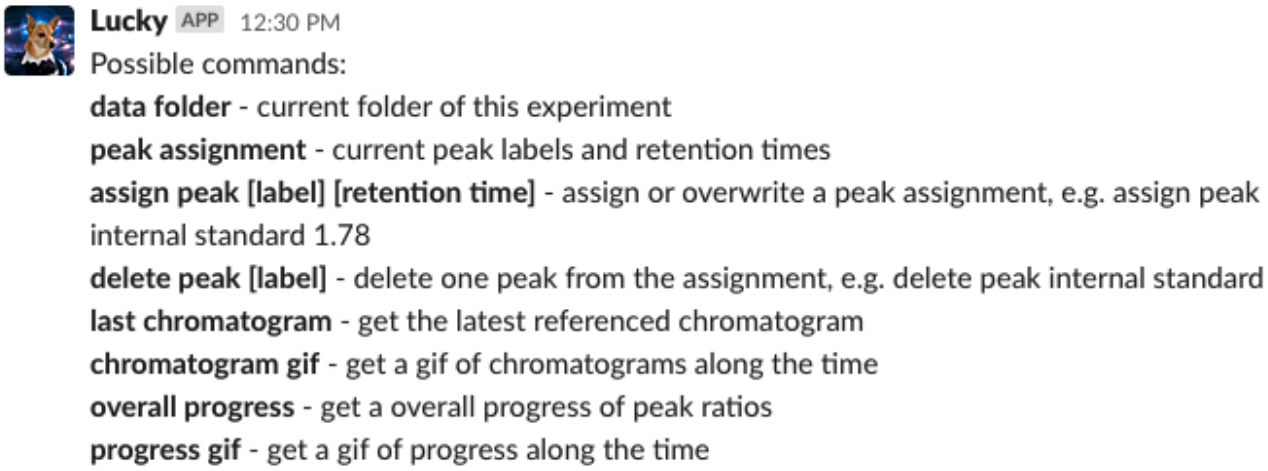

Figure 15: A list of available keyword commands for HPLC reaction monitoring

Figure 12 shows a list of the keywords commands that are used for the HPLC reaction monitoring. The purpose of integrating Slack with this reaction platform is to remotely obtain the current experimental status and visualize the experimental data. Using the chromatogram keywords, the experimenter can read the existing referenced HPLC output (e.g., *Figure 11*) via Slack with each peak labelled by its name. The peak labels can be shown and modified using the peak assignment keywords. In addition, we want to visualize the concentration of each compound as time progresses.

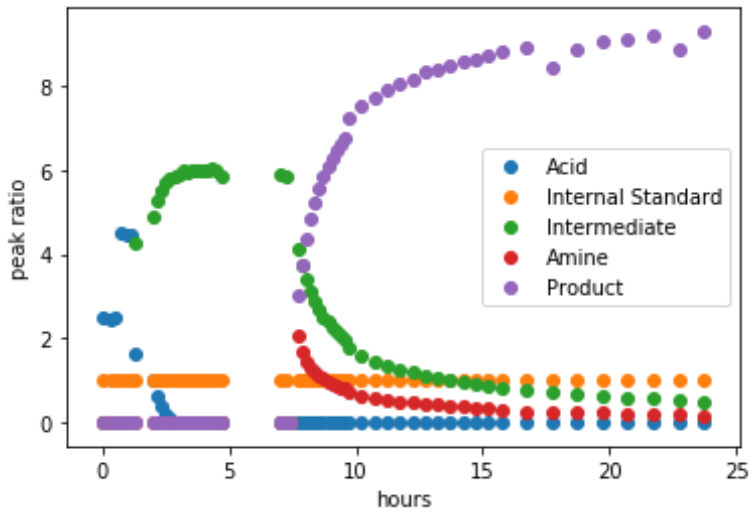

Figure 16: Example overall progress of carboxylic acid and amine coupling

Figure 13 is the visualization of an example run of carboxylic acid and amine coupling. To account for the overall volume loss due to each sampling, we used an internal standard and normalized the peak integrations of the reacting substances with respect to the peak integration of the internal standard. Data collected before the 5-hour point indicates the first step of the reaction, and data after the 5-hour time point is the CDI quenching and the second step of the reaction. We observe during the first step, the carboxylic acid is first added and gradually consumed, shown by the increase and decrease of the blue dots. At the same time, we see the acyl imidazol intermediate is formed, shown by the increase of the green dots. During the second step, we see an amount of amine is dosed, and the peak ratio of amine decreases along with the intermediate peak integration. At the same time, the purple amide product is formed, shown by the increase of the purple dots. The system terminates around 24 to 25 hours of reaction, signalled by the relative constant amide-to-internal-standard peak ratio. This constant ratio indicates that the reaction rate of the amide is slow, and the system is approaching equilibrium. The progress keywords in Slack allow the experimenter to obtain this progress report, thus, to understand the status of the reaction.

3.3.3 Discussion

The presented HPLC direct-inject platform and HPLC data analysis algorithm allows the experimenter to perform amide bond formation experiments using carbonyldiimidazole activation. Vial movements and reagent dosing are achieved using the robotic arm. The reaction is monitored using peak information acquired from the looped sampling sequence. The sampling sequence is constructed using the combination of liquid handling module, HPLC instrument, and the robotic arm. The data produced by the HPLC is further analyzed using a self-developed algorithm that is capable of detecting and integrating peaks. The peaks are detected by significantly high intensity and its surroundings compared to the referenced baseline, and the retention time of the peak is the time point corresponding to the local

maximum intensity. The integration of the peak area is calculated by highly accurate numerical approximations of the data curve. Since retention times are the characteristic for each substance, each detected peak is labelled with the associated substance name along with the reaction progress by the algorithm. This platform runs automatically after the first initialization; with the HPLC monitoring, the system understands the progress of the reaction and decides accordingly on the next instrumental command.

Using this automated platform for this amide bond formation reaction brings multiple benefits to the productivity, understanding, and research applicability of amide bond formation. Results previously shown suggested that the entire reaction may take over 24 hours. Being able to automatically run the reaction and sampling saves a significant amount of research attention and time, which could be utilized for other research purposes. Unlike researchers who attend laboratories in a limited amount of time per day, the platform is active 24 hours. Thus, using the platform, we can execute the experiment during off-hours as well as the sampling. Since physical presence is not required from the researcher and the system is remotely accessible from Slack, the experimenter can acquire reaction data anywhere over the internet.

Different from traditional overnight reactions, we understand the progress of the reaction at each time point. Traditionally, overnight reaction under constant stirring only does not provide sufficient information of the reaction progress due to the lack of analysis during the night. By automatic HPLC sampling, we acquire the samples as time progresses and dynamically visualize the reaction data. This allows us to clearly see the reaction rate, present substances, and duration of individual reaction steps, which gives us a thorough understanding of reaction kinetics and dynamics.

With the capability of HPLC monitoring, the system can perform the carboxylic acid and amine coupling independent of the types of the carboxylic acid and amine. Providing that CDI activation is a

viable synthetic route for the starting materials, the system can couple the acid and amine with arbitrary R groups. Thus, the desired amide can be synthesized if the corresponding starting materials are used. Together with the automation, this platform presents as a powerful tool on amide bond synthesis via CDI activation.

3.3.4 Limitations

Despite the capabilities of this system, there is a list of limitations and prospective modifications that we can further improve this system. Firstly, the computational effort for data visualization is long. While processing one HPLC sampling data takes only 2 seconds, to construct an overall progress plot (e.g., *Figure 13*), which may contain up to 60 data points, takes up to 2 minutes. Furthermore, generating a data visualization that dynamically presents all data points in a graphic interchange format (GIF) consumes up to one hour of the computational time. A more efficient algorithm is needed to shorten the computational time of data visualization. Secondly, the algorithm requires clear peak separations of each substance. Partial, or complete peak overlaps are accompanied by a natural data loss. If the peaks are not distinctly separated, the current algorithm classifies overlapped peaks as one single peak, which may result in false peak assignments and integration. While properly selecting the mobile phase assists in peak separation, in the future, mathematical tools can be employed to calculated partially overlapped peaks utilizing the symmetry of the peaks. Finally, the system is limited to the synthetic route of amide bond formation using CDI as the coupling reagent. Currently, our system is not applicable to other syntheses of amide bond formation. However, we have the tools and experimental actions needed to move vials, dose reagent, and take HPLC sampling. The workflow can be easily adapted to other synthetic routes providing their experimental procedures.

4. CONCLUSION

In this technology report, we present two different designs of automated robotic platforms using modular programmable laboratory instruments integrated by a seven-axis articulated robotic arm. These robotic platforms individually provide real-time monitoring in a qualitative and a quantitative approach. In the qualitative approach, we developed a titration-like solubility testing workflow that employs a computer vision module for the measurement of turbidity based on the graphical feedback. In the quantitative approach, we designed auto-HPLC sampling sequences to drive arbitrary carboxylic acid and amine coupling using carbonyldiimidazole activation. Since these experiments involve conditional choices of procedure execution, we programmed analysis scripts to interpret the status of the system so that the workflow becomes self-driven. In addition, we developed a laboratory assistant using Slack to allow researchers to remotely access the system and acquire the real-time experimental state after the first initialization. The platforms are currently limited in the applicability to a wider range of analytes and future work will be focused on adaptation of coloured substances for solubility, and novel reaction procedures for HPLC monitoring.

5. REFERENCES

1. Yang, F.; Lai, V.; Legard, K.; Kozdras, S.; Prieto, P. L.; Grunert, S.; Hein, J. E. Augmented Titration Setup for Future Teaching Laboratories. *J. Chem. Educ.* **2021**. https://doi.org/10.1021/acs.jchemed.0c01394.
2. Armbruster, D. A.; Overcash, D. R.; Reyes, J. Clinical Chemistry Laboratory Automation in the 21st Century - Amat Victoria Curam (Victory Loves Careful Preparation). *Clin. Biochem. Rev.* **2014**, *35* (3), 143–153.
3. MacLeod, B. P.; Parlane, F. G. L.; Morrissey, T. D.; Häse, F.; Roch, L. M.; Dettelbach, K. E.; Moreira, R.; Yunker, L. P. E.; Rooney, M. B.; Deeth, J. R.; Lai, V.; Ng, G. J.; Situ, H.; Zhang, R. H.; Elliott, M. S.; Haley, T. H.; Dvorak, D. J.; Aspuru-Guzik, A.; Hein, J. E.; Berlinguette, C. P. Self-Driving Laboratory for Accelerated Discovery of Thin-Film Materials. *Sci. Adv.* **2020**. https://doi.org/10.1126/sciadv.aaz8867.
4. Tan, S. W. B.; Naraharisetti, P. K.; Chin, S. K.; Lee, L. Y. Simple Visual-Aided Automated Titration Using the Python Programming Language. *J. Chem. Educ.* **2020**, *97* (3), 850–854. https://doi.org/10.1021/acs.jchemed.9b00802.
5. Hill, B. G.; Benavides, G. A.; Lancaster, J. J. R.; Ballinger, S.; Dell'Italia, L.; Zhang, J.; Darley-Usmar, V. M. Integration of Cellular Bioenergetics with Mitochondrial Quality Control and Autophagy. In *Biological Chemistry*; 2012. https://doi.org/10.1515/hsz-2012-0198.
6. Malig, T. C.; Koenig, J. D. B.; Situ, H.; Chehal, N. K.; Hultin, P. G.; Hein, J. E. Real-Time HPLC-MS Reaction Progress Monitoring Using an Automated Analytical Platform. *React. Chem. Eng.* **2017**. https://doi.org/10.1039/c7re00026j.

7. Collins, J.; Howard, D.; Leitner, J. Quantifying the Reality Gap in Robotic Manipulation Tasks. In *Proceedings - IEEE International Conference on Robotics and Automation*; 2019. https://doi.org/10.1109/ICRA.2019.8793591.

8. Li, J.; Sun Lee, W.; Hsu, D. Push-Net: Deep Planar Pushing for Objects with Unknown Physical Properties; 2018. https://doi.org/10.15607/rss.2018.xiv.024.

9. Campeau-Lecours, A.; Lamontagne, H.; Latour, S.; Fauteux, P.; Maheu, V.; Boucher, F.; Deguire, C.; L'Ecuyer, L.-J. C. Kinova Modular Robot Arms for Service Robotics Applications. *Int. J. Robot. Appl. Technol.* **2018**. https://doi.org/10.4018/ijrat.2017070104.

10. Shiri, P.; Lai, V.; Zepel, T.; Griffin, D.; Reifman, J.; Clark, S.; Grunert, S.; Yunker, L. P. E.; Steiner, S.; Situ, H.; Yang, F.; Prieto, P. L.; Hein, J. E. Automated Solubility Screening Platform Using Computer Vision. *iScience* **2021**. https://doi.org/10.1016/j.isci.2021.102176.

11. Velasco, J. B.; Knedeisen, A.; Xue, D.; Vickrey, T. L.; Abebe, M.; Stains, M. Characterizing Instructional Practices in the Laboratory: The Laboratory Observation Protocol for Undergraduate STEM. *J. Chem. Educ.* **2016**. https://doi.org/10.1021/acs.jchemed.6b00062.

12. Coltescu, A.-R.; Butnariu, M.; Sarac, I. *Biomedical and Pharmacology Journal.* **2020**, *13*(02), 577–583. https://dx.doi.org/10.13005/bpj/1920

13. Hansen, C. M. 50 Years with Solubility Parameters - Past and Future. *Prog. Org. Coatings* **2004**. https://doi.org/10.1016/j.porgcoat.2004.05.004.

14. MacHui, F.; Abbott, S.; Waller, D.; Koppe, M.; Brabec, C. J. Determination of Solubility Parameters for Organic Semiconductor Formulations. *Macromol. Chem. Phys.* **2011**. https://doi.org/10.1002/macp.201100284.

15. Walker, B.; Tamayo, A.; Duong, D. T.; Dang, X. D.; Kim, C.; Granstrom, J.; Nguyen, T. Q. A Systematic Approach to Solvent Selection Based on Cohesive Energy Densities in a

Molecular Bulk Heterojunction System. *Adv. Energy Mater.* **2011**. https://doi.org/10.1002/aenm.201000054.

16. Hoelke, B.; Gieringer, S.; Arlt, M.; Saal, C. Comparison of Nephelometric, UV-Spectroscopic, and HPLC Methods for High-Throughput Determination of Aqueous Drug Solubility in Microtiter Plates. *Anal. Chem.* **2009**. https://doi.org/10.1021/ac9000089.
17. Valeur, E.; Bradley, M. Amide Bond Formation: Beyond the Myth of Coupling Reagents. *Chem. Soc. Rev.* **2009**. https://doi.org/10.1039/b701677h.
18. Roughley, S. D.; Jordan, A. M. The Medicinal Chemist's Toolbox: An Analysis of Reactions Used in the Pursuit of Drug Candidates. *Journal of Medicinal Chemistry*. 2011. https://doi.org/10.1021/jm200187y.
19. Staab, H. A. New Methods of Preparative Organic Chmistry IV. Syntheses Using Heterocyclic Amides (Azolides). *Angew. Chemie Int. Ed. English* **1962**. https://doi.org/10.1002/anie.196203511.
20. Armstrong, A.; Li, W. N,N ′-Carbonyldiimidazole . In *Encyclopedia of Reagents for Organic Synthesis*; 2007. https://doi.org/10.1002/9780470842898.rc024.pub2.
21. Karger, B. L. HPLC: Early and Recent Perspectives. *Journal of Chemical Education*. 1997. https://doi.org/10.1021/ed074p45.
22. Hanlan, J.; Skoog, D. A.; West, D. M. Principles of Instrumental Analysis. *Stud. Conserv.* **1973**. https://doi.org/10.2307/1505543.
23. Foley, D. A.; Wang, J.; Maranzano, B.; Zell, M. T.; Marquez, B. L.; Xiang, Y.; Reid, G. L. Online NMR and HPLC as a Reaction Monitoring Platform for Pharmaceutical Process Development. *Anal. Chem.* **2013**. https://doi.org/10.1021/ac402382d.

24. Tang, N.; Toriba, A.; Kizu, R.; Hayakawa, K. Improvement of an Automatic HPLC System for Nitropolycyclic Aromatic Hydrocarbons: Removal of an Interfering Peak and Increase in the Number of Analytes. *Anal. Sci.* **2003**. https://doi.org/10.2116/analsci.19.249.

25. Zepel, T.; Lai, V.; Yunker, L. P. E.; Hein, J. E. Automated Liquid-Level Monitoring and Control Using Computer Vision. *ChemRxiv*. 2020. https://doi.org/10.26434/chemrxiv.12798143.v1.

26. Liu, Y.; Chen, Y.; Fang, X. A Review of Turbidity Detection Based on Computer Vision. *IEEE access* **2018**, *6* (Journal Article), 60586–60604. https://doi.org/10.1109/access.2018.2875071.

27. Fitzpatrick, D. E.; Battilocchio, C.; Ley, S. V. A Novel Internet-Based Reaction Monitoring, Control and Autonomous Self-Optimization Platform for Chemical Synthesis. *Org. Process Res. Dev.* **2016**. https://doi.org/10.1021/acs.oprd.5b00313.

6. APPENDIX

6.1. Overview

To construct the automated robotic platform of reaction monitoring, we integrated programmable hardware with individual functionality that reduces the need for human intervention. The robotic motions of the programmable hardware equivalently achieve necessary manual operations from an experimenter, such as glassware movement, solid and liquid handling, effective mixing, and temperature control. Each hardware is designed to be able to independently perform one or more elementary procedures. The integration of the hardware sequentially arranged by workflow algorithm collaborates to accomplish one experimental goal, and this modular design enables easy adaptation and reconfiguration for changing experimental needs.

6.2. General Deployed Instruments and Programming Methods

6.2.1 Kinova Robotic Arm and End Effector

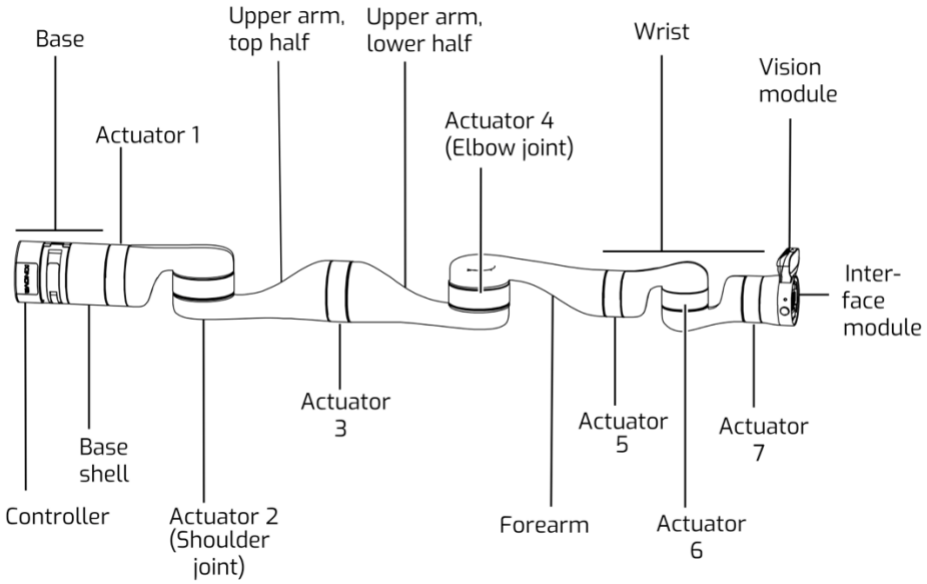

Figure 17: Diagram of the Kinova Gen3 robotic arm

We selected Kinova Gen3 modular robotic arm combining Robotiq 2F-85 gripper for movement of reactors and other hardware. The Kinova Gen3 is a seven-axis articulated arm with a maximum of seven-kilogram payload. The flexibility, dexterity, and reach of multiple articulated components allow Kinova to handle challenging tasks that span on non-parallel planes. Each of the seven actuators offers 360-degree rotation that supports precise operations in narrow space and free movements inside of a hemisphere with a maximum reach of one meter.

The arm's movements are programmed using the Kinova Web Application and the HeinRobot control library. We first manually move the arm to the desired locations, then encode the three-dimensional Cartesian and angular positions of the arm into the JavaScript Object Notation (JSON) format using the Kinova Web Application. In the Python programming language, using the HeinRobot supports the arm translating between arm positions. To avoid collisions from itself or other hardware, stepwise design of robotic motions is often applied.

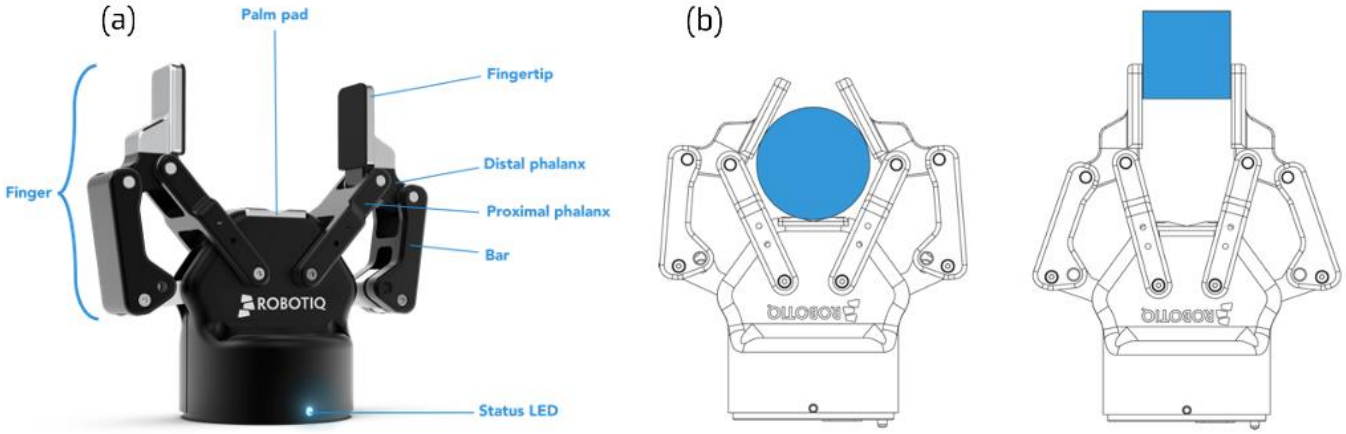

Figure 18: (a) Diagram of the Robotiq 2F-85 gripper. (b) Gripping positions while handling objects with different geometry

We selected the Robotiq 2F-85 gripper (*Figure 15[a]*) connected to the interface module of the arm. The gripping force is provided by the distal and proximal phalanx, and the default fingertips are detachable. The detachability of the fingertips allows for custom-designed gripping fingers, which can be

modified to transfer, cap, and uncap vials of various sizes. Also, the phalanx design provides advanced flexibility in handling cylindrical and rectangular objects (*Figure 15*[b]), such as vials and the liquid handler - the Samplematic.

6.2.2 Liquid Handling Module

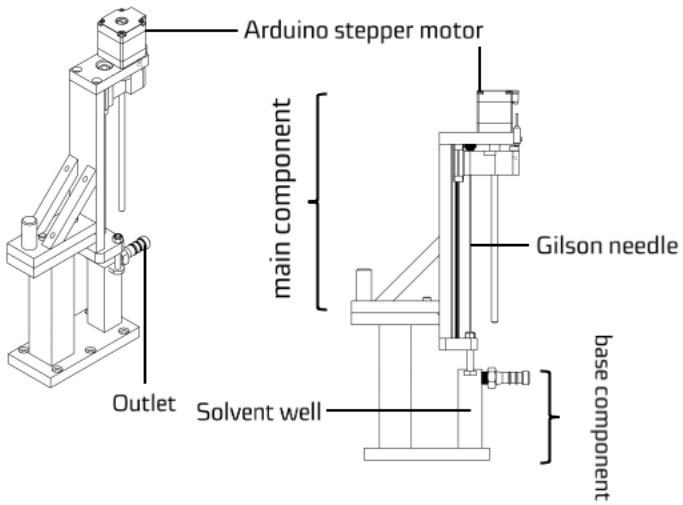

Figure 19: Diagram of the Sampleomatic

To satisfy the need for liquid withdrawal and injection, we designed the automated liquid handler, the Sampleomatic (*Figure 16*). The Sampleomatic consists of a main component and a base component. The main component consists of an Arduino stepper motor and a Gilson titanium dispense needle. While being lifted and brought to the desired vial location by the robotic arm, the Arduino stepper motor drives the needle down to reach inside of the reaction vial through septum caps. This allows the reacting mixture to be isolated from the atmosphere, hence avoiding side reaction and solvent evaporation. When the Sampleomatic is unoccupied, it is located on the base for self-rinsing. The base consists of a well underneath the needle tip. The stepper motor drives down the needle into the well to allow a sufficient amount of solvent to flush through the needle to give a thorough rinse for inline and the needle tip

preparing for subsequential liquid dosing. The waste liquid is being drained through the outlet while flushing.

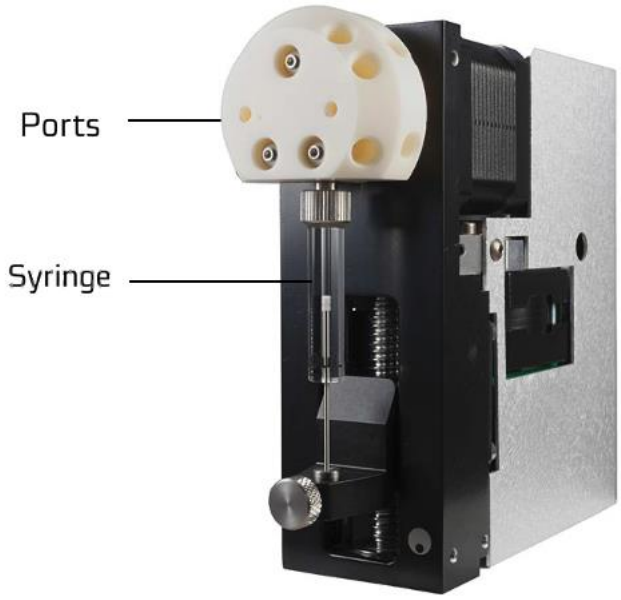

Figure 20: Diagram of the Tecan Cavro syringe pump

We used the Tecan Cavro syringe pump for the main liquid movement driving force. The Tecan Cavro syringe pump dispenses, pipettes, and dilutes with high precision and accuracy using a variety of syringe sizes. It supports 5-microlitre to 5-mililitre dosage with a flow rate of up to 20 millilitres per minute. The hardware and software design promotes durability and reduces the need for further maintenance and calibration. It consists of three selectable ports for dispensing and withdrawing, driven by the pressure difference between the syringe and atmosphere. We developed the NorthRobotics Python library for syringe pump control, enabling remote control of liquid transfer by pumping from the solvent port and pushing to the needle of the Sampleomatic.

6.2.3 Solid Handling Module

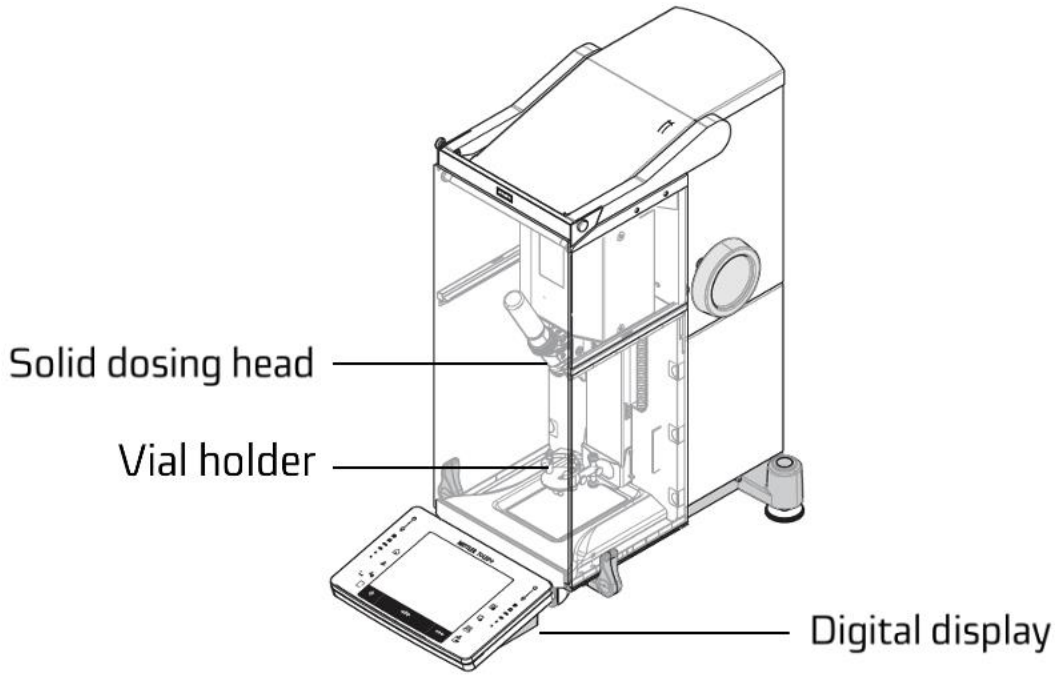

Figure 21: Diagram of the Metter Toledo Quantos

We used Mettler Toledo Quantos for solid weighing and dosing (*Figure 18*). Quantos is an automated dosing balance that provides accurate powder dosing within 1-milligram range from the desired mass. The solid is contained in a dosing head that is free to be driven vertically inside Quantos. An Arduino stepper motor is augmented with the Quantos for automatic dosing head movement. After placing an uncapped vial inside Quantos, the Arduino stepper motor drives the dosing head down to reach the top opening of the vial. Then, small portions of solid powder are consecutively dosed into the vial while the Quantos monitors the real-time mass of the vial. Once the mass has increased over the desired amount, the dosing hand is driven up, creating space for retraction of the vial by the arm. In case that alternative chemicals are needed, a holder that contains multiple dosing heads is employed and the robotic arm achieves the swapping of dosing heads.

6.3 Instrumental Setup for Qualitative Monitoring

Solubility testing serves as a great example of how qualitative determination can be advantageous in an experimental procedure. The dissolution of the solute is reflected by the turbidity of the solid-liquid mixture. Thus, graphical feedbacks are essential for the computer to determine the dissolving progress. In order to acquire the graphical feedbacks, a vision station (*Figure 19*) is designed for monitoring the turbidity from the side view of the vial. The vision station consists of two available HPLC-vial-sized positions, which are inside of the frame of a webcam. One position is for a clear dissolved reference, and the other position is for the heterogeneous dissolving mixture. Placing the dissolved reference aside the dissolving mixture reduces the ambient light effect on turbidity measurement while analyzing by the computer vision algorithm.

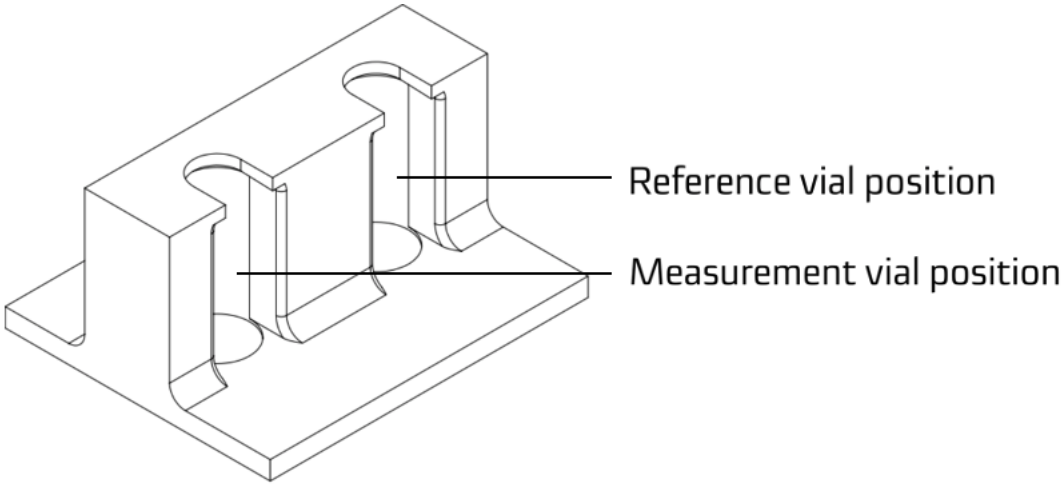

Figure 22: Diagram of the vision station

To provide a sufficient mixing condition, we deployed an IKA stir plate under the vision station. The IKA stir plate is a programmable magnetic stirrer that rotates the magnetic stir bar we pre-dosed in the vial. The Python IKA library provides advanced control to ensure the stir bar activity does not interfere with the computer vision algorithm.

The solubility test of a substance often involves multiple solvents. Thus, a variety of solvent selections are integrated into the liquid handling module. *Figure 20* shows that the Tecan Cavro syringe pump connects the Sampleomatic and a 10-port VICI valve. The VICI valve is a programmable selection valve that is able to connect any of the secondary ports to the main port. At the beginning of each liquid dosing, the VICI valve is switched to the port connecting to the desired solvent; then, the syringe pump pumps sufficient solvent to prime the line and wash the needle.

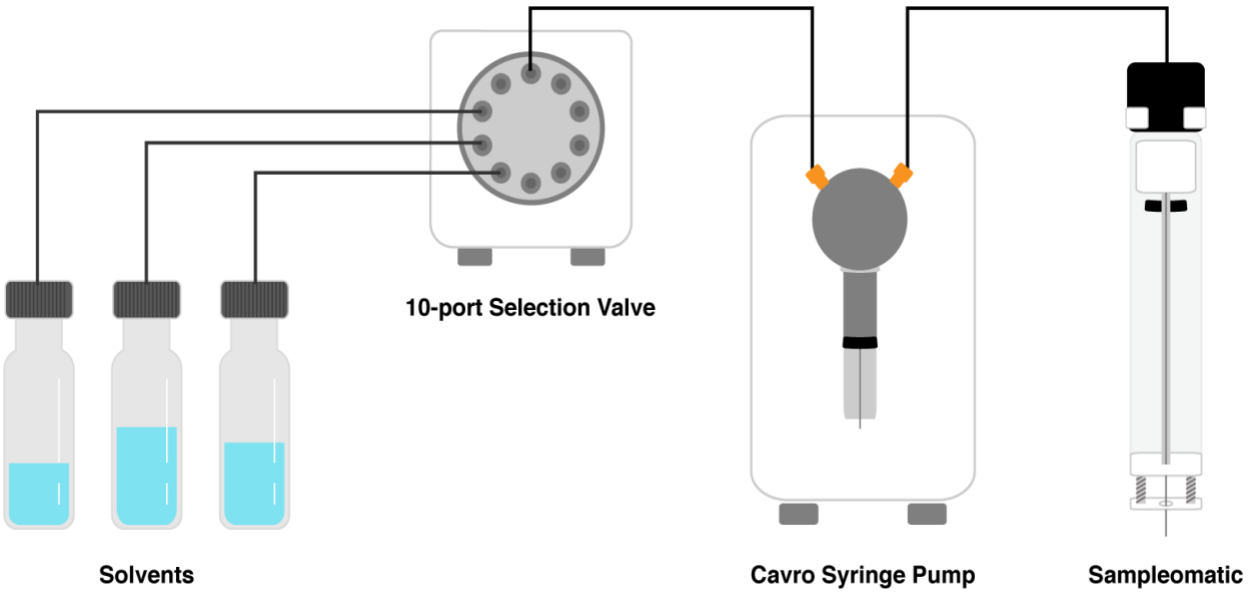

Figure 23: Diagram of the liquid handling module

Since solubility testing is a volume-sensitive procedure, we aspire for an isolated dissolving condition to prevent solvent evaporation. While usage of septum caps is convenient for liquid injection, uncapping action is still inevitable considering the necessity of automatic solid dosing. We designed a gripper station (*Figure 21*) to secure the position of the vial while the robotic arm is uncapping. In between the 3D printed board and a vial holder, we inserted an O-ring to provide enough friction to the glass part of the vial while the robotic arm is rotating the cap. While handling the uncapped vial, the cap is placed on the top of the screw used to secure the plastic board (*Figure 21*^{b}).

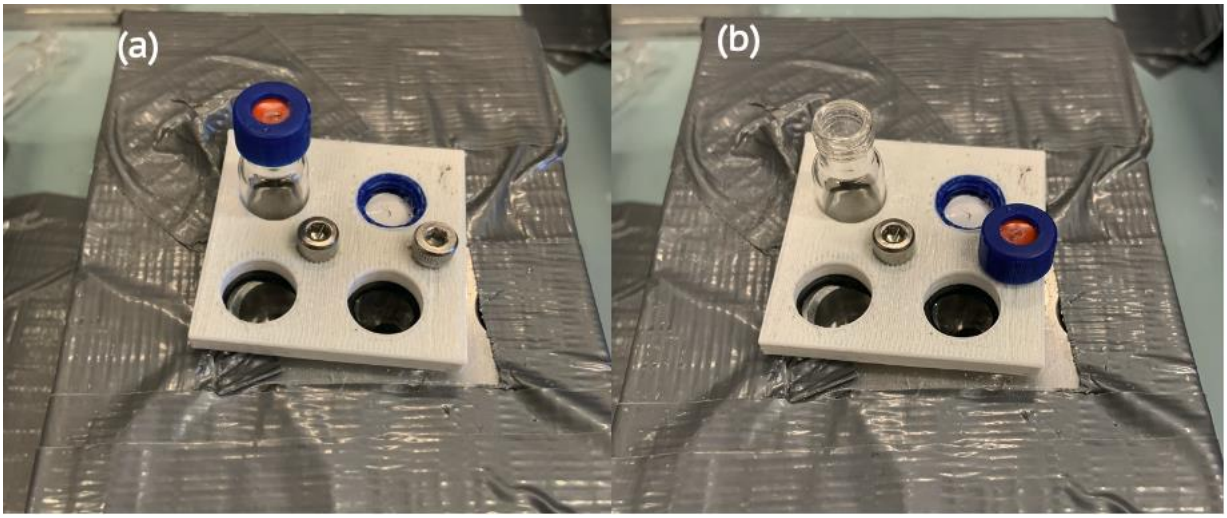

Figure 24: (a) Capped vial position. (b) Uncapped vial and cap position

Due to the limited free-moving space available for different hardware, the robotic arm needs to be oriented vertically and horizontally, respectively on the vial deck and inside of the Quantos. To allow the switching of arm orientation, we designed the regripping station for the temporary vial holder while the arm is changing between vertical and horizontal position. The regripping station provides the flexibility of vial intake angle to reduce instrumental location displacement and appropriate height to prevent collisions of the hardware. *Figure 22*[a] shows the approximate location of the regripping station and other modules for solubility test on a diagram, and *Figure 22*[b] shows the setup of the deck in real life.

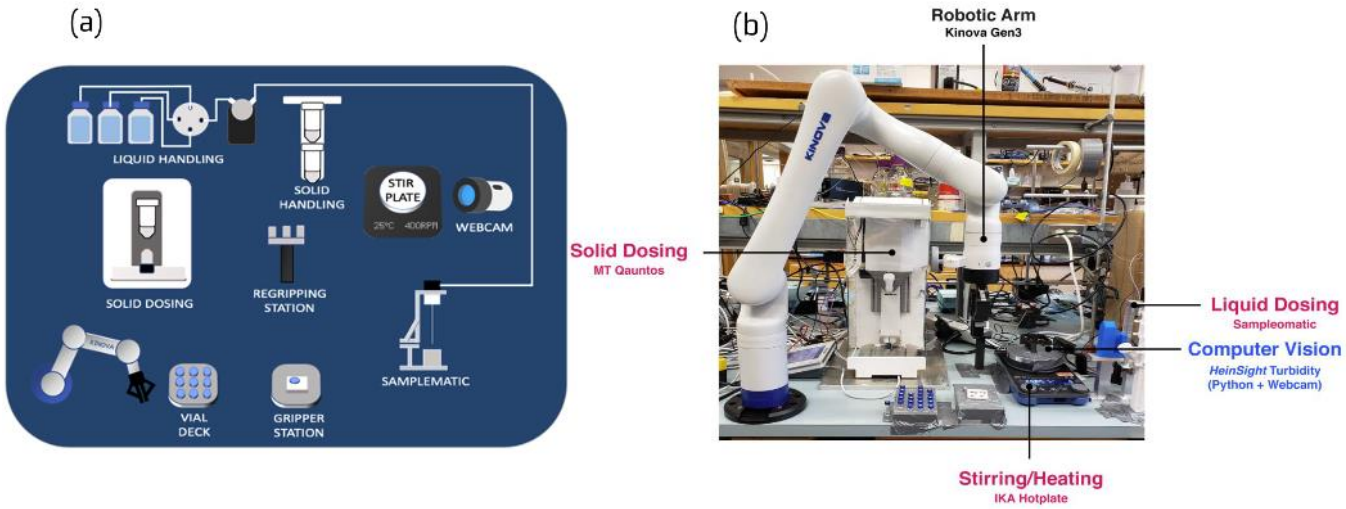

Figure 25: (a) Diagram of the solubility deck. (b) Solubility deck in real life.

6.4 Instrumental Setup for Quantitative Monitoring

Since visual access is no longer necessary in the quantitative analysis, we deployed Electrothermal Integrity 10 as the reaction station. Integrity 10 is a ten-position reaction station that features separated temperature and stir rate control for each individual position. In each position, the vial is surrounded by a metal container whose temperature is regulated by an external heater and chiller. A magnetic field is also generated to support a custom stir rate. In the workflow, the robotic brings the reactor, which has been pre-dosed with a stir bar, into an available position. The corresponding position is activated to maintain a constant temperature of 25 °C and a stir rate of 500 RPM during the entire course of the reaction.

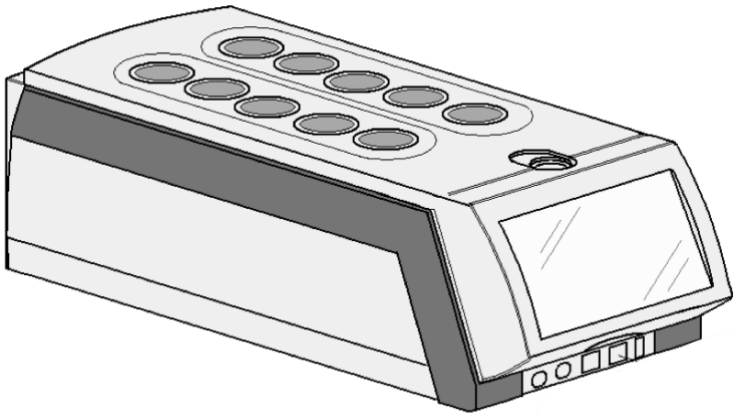

Figure 26: Diagram of Integrity 10

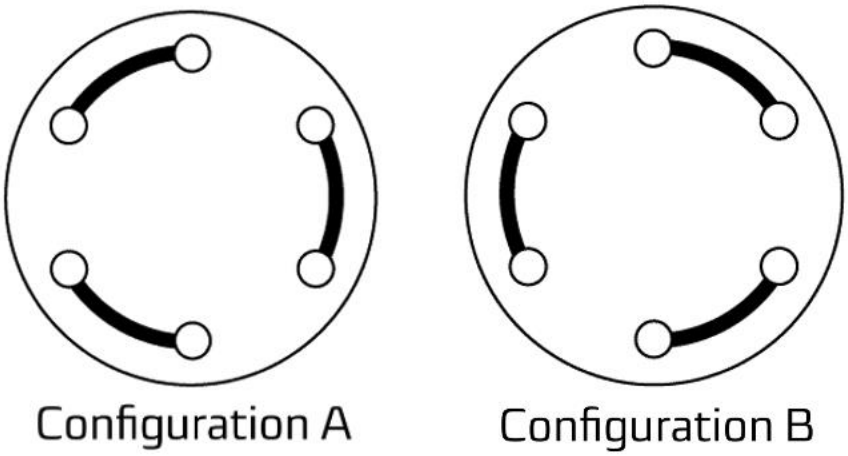

Figure 27: Two configurations of the 6-port VICI valve

To automate the HPLC injection process, we used the VICI 6-port selection valve. The VICI valve consists of two configurations (*Figure 24*). Each configuration connects two complemental adjacent ports. We developed the VICI python package to switch between these two positions. (*Figure 25*) shows how we utilized the selection valve to make the HPLC sample. First, the robotic arm brings Sampleomatic to the reactor to take a small amount of the reaction mixture. We calibrate the travel length so that the sample passes port 1,6,3,2 and fills the entire sample loop. Then, the VICI vial switches from position A to position B. A second syringe pump connecting to port 4 pushes the mobile

phase through port 4,3,6,5 and enters the column. The mobile phase dilutes the sample and enters the column at port 5 for the HPLC analysis afterward.

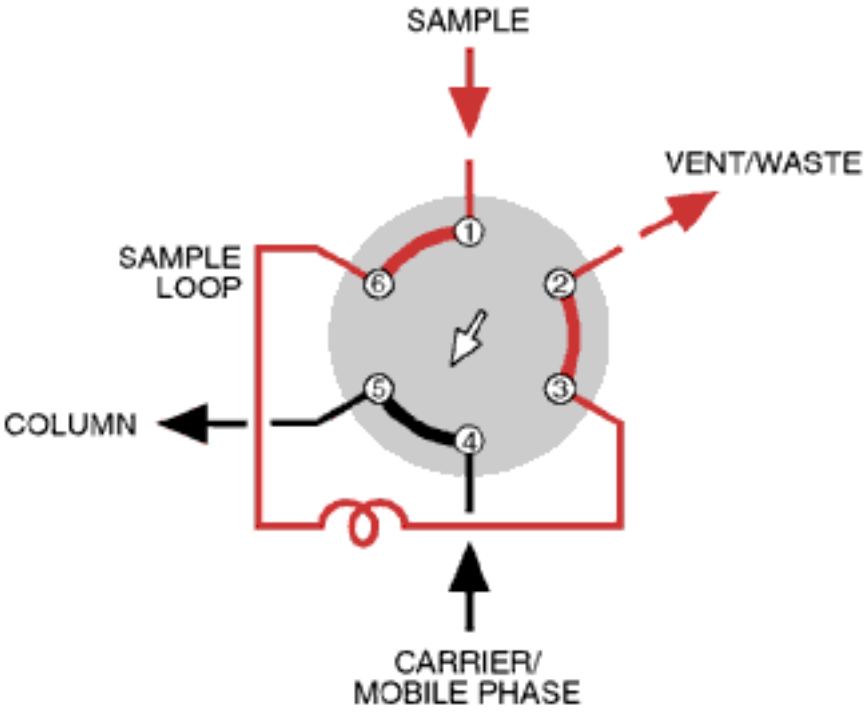

Figure 28: Direct-inject sample flow